Bull. Astr. Soc. India (1983) 11, 104–114

NOTES FOR THE OBSERVER

by T. P. Prabhu

1. Solar physics in the nineteenth century

The sun, which sustains life, regulates the day and night and seasons, has always been the most important celestial object for mankind. For all visual apperances, the sun goes around the earth every day and at a slightly refined level of observations, moves with respect to stars completing a revolution in one year. While some of the ancient philosophers placed the sun at the centre of the universe, early crude measurements could easily be made to fit a geocentric system in which the sun, the moon and the planets revolved around the earth. The occasional retrograde motion of the outer planets could be explained by Ptolemaic epicycles on the orbits. As the observations improved in accuracy, the geocentric theory demanded epicycles over epicycles in order to agree with observations. Finally, Nicolas Copernicus showed that a heliocentric system explains the observations in much simpler terms.

When Galileo and others turned the telescope towards sky, it was seen that all planets are globes like earth, and some planets had their own moons. The sun was seen to have black spots over its face. Continued observations of these spots showed that the sun too rotated like the planets. Even until the end of the eighteenth century, it was believed that the only difference between the planets and the sun was the enormous mass of the sun and its incandescent atmosphere. Sunspots were thought variously to be volcanic mountains rising above the luminous clouds, or dark clouds of accumulated slag. After Alexander Wilson (1774) noticed that the sunspots appear as depressions in the solar photosphere, William Herschel (1795) speculated that they are holes in the layers of clouds through which cool surface of the sun could be seen, and this surface could even be inhabited.

It was realized by the middle of the nineteenth century that things were not as simple as that. The amateur astronomer S. H. Schwabe (1843) showed that the number of sunspots varied with a period of ten years. A decade later, Lamont, Sabine, Wolf and Gautier noticed that the magnetic field of earth also varied with the same period, though the causal connection was not at all clear. Reasonably accurate value for the radiation received from the sun (the so-called solar constant) also became available only at this time thanks to John Herschel, C. S. M. Pouillet and J. D. Forbes. These measurements could be used to derive the temperature of the sun. However, no empirical relation was known between the amount of radiation and such a high temperature; an extrapolation from the laboratory data yielded a mere 1750 C for the sun's temperature. The prominences and the corona were also observed around the midcentury. High resolution Fraunhofer spectra were also available. The ideas in spectral analysis crystallized through the monumental work of Kirchhoff (1853); and the Doppler-Fizeau effect (1842–1848) was theoretically postulated. Daguerreotypes could be used to record the images for subsequent objective evaluation. Thus the stage was set for expanding the human perception.

The first indication that the age of the solar system is longer than a few million years came from the geological evidences. The question about the source of solar energy was thus posed. J. R. Mayer's suggestion of impact of meteorites over the solar surface did not receive any support, since it led to an appreciable increase in the mass of the sun, which should have resulted in a gradual change in earth's orbit and consequently in the seasons. Hermann von Helmholtz suggested in 1854 that the sun shone owing to the release of gravitational energy by contraction. This theory prevailed for a long time. An improvement in geological dating took place only after the discovery of radioactivity whereas an understanding of the source of solar energy had to await the advent of nuclear physics.

The phenomena on or above the solar surface, discovered and studied during the nineteenth century, include the solar flares, chromospheres, prominences and the corona. The solar flares were discovered by R. C. Carrington & R. Hodgson in 1859 as two bright patches over a sunspot which lasted for about five minutes. Such flares were more commonly observed spectroscopically since the seventies as a sunspot moved over the solar limb. A terrestrial magnetic storm was already witnessed coinciding with the white light solar flare observed by Carrington & Hodgson. The accumulated data on chromospheric flares increasingly supported the idea that the causal connection between the solar and terrestrial activity is provided by these flares.

The study of the chromosphere, prominences and the corona progressed rapidly during the second half of the nineteenth century mainly due to the observations of solar eclipses (see *Bull. Astr. Soc. India* **10**, 252, 1982). The method of spectral analysis was also taking great strides during this period. Furthermore, it was realised that much important work could be accomplished even when the sun was not eclipsed. P. J. C. Janssen and J. N. Lockyer discovered in 1868 that the porminences could be studied spectroscopically without waiting for the solar disk to be eclipsed G. E. Hale constructed the spectroheliograph in 1889, which could provide monochromatic images of the sun with the highest spectral purity. These images could be used to photograph prominences (in H_α light) and the chromosphere (in Ca II K). The first attempt to photograph solar corona without an eclipse was made by William Huggins in 1882. Coelostats were used by H. H. Turner in 1896 to feed light to a fixed telescope allowing a greater rigidity to the telescope and spectrograph. Thus at the end of the nineteenth century an urgency was felt by astronomers for full-fledged solar observatories where observations of the highest resolution could be obtained on a routine basis.

Three major mountain-top solar observatories started functioning at the turn of the century. The first of these was Meudon observatory founded by Janssen in 1875; Kodaikanal observatory was set up in 1899 by Michie Smith, and Mount Wilson solar observatory, founded by Hale, was soon to follow (1904). The results were certainly rewarding. Important discoveries that followed were the solar granulation of Janssen (1879) at Meudon, the magnetic field of sunspots by Hale (1908) at Mount Wilson, and the radial motions in sunspots by Evershed (1909) at Kodaikanal.

2. Signal-to-noise ratio of photographic emulsions

Photographic emulsion is a two-dimensional storage device of information on the amount of incident light. When one wants to read out this information, one would

like to know the precision with which one can identify the location at which the information is stored, and the noise added by the system to the information. The positional precision becomes important in applications like astrometry, and radial velocity measurements while the precision with which the incident intensity can be estimated is more important in photometric applications.

If the calibration curve for a photographic plate is determined accurately, one should, in principle, be able to obtain the relative incident intensity from the measured density. However, if we record several constant exposures on a photographic emulsion, it would not reach exactly the same density every time because of the granularity of the plate. One may assume reasonably well that the density D registered by the plate for a given exposure E follows a normal distribution around mean D with a standard deviation σ_D. The exposure inferred from a given D would then be E with the uncertainty σ_E corresponding to σ_D in the density domain. Here, E is the signal and σ_E the noise introduced by the photographic emulsion. If one defines the slope of H—D curve at a given density as

$$dD/d\,(\log E) = \gamma,$$

one may write

$$\frac{\sigma_D}{\sigma_E} = \frac{dD}{dE} = \frac{dD}{Ed\,(\ln E)}$$

$$= \frac{0.434}{E}\,\frac{dD}{d(\log E)}$$

$$= \frac{0.434\gamma}{E}.$$

Hence the signal-to-noise (S/N) ratio is

$$\frac{E}{\sigma_E} = \frac{0.434\gamma}{\sigma_D}.$$

This is called the *output* signal-to-noise ratio and quantifies the precision with which the exposure can be determined for a given slope γ of the H—D curve and given density noise σ_D. The most general formula for this noise is

$$\sigma_D\,(l) = \left\{ \frac{\sum_{i=1}^{N-1} [D(x_i) - D(x_i + l)]^2}{2(N-1)} \right\}^{\frac{1}{2}}$$

where x_i and $x_i + l$ are two positions on the photographic plate separated by a distance l, in a linear scan.

The above equation gives the complete spectrum of noise as a function of length scale l. In practice, one gives a uniform exposure and uses the string of densities digitized at a constant interval Δx which is smaller than the grain size of the emulsion. The noise spectrum is calculated for $l = n\Delta x$. This spectrum has nearly a constant value for small values of l ($\lesssim$ 1 mm), but the noise increases steadily for large l because of the large-scale inhomogeneities of the emulsion. In most of the astronomical applications, one is generally interested in the local noise (small l; say, $l = \Delta x$). This noise has been termed as micronoise against macronoise which is

evaluated simply as the root-mean-square deviation of the densities from their local mean value :

$$\sigma_D(\text{macro}) = \frac{1}{N} \sum_{j=1}^{N} [\bar{D} - D(x_i)]^2.$$

The micronoise and macronoise would be equal to each other when the mean density level is constant, that is, when the inhomogeneities of longer lengthscales are absent.

The grain noise of a photographic plate increases with increasing density (figure 1a). Thus while the S/N can be improved by integrating longer with the photoelectric devices, it is not always possible to do so with a photographic detector. As one increases the exposure time, the S/N of a photographic record increases to a maximum value around the diffuse density 1 (depending on the emulsion, hypersensitization *etc.*) and falls down thereafter (figure 1b). Hence one needs to optimize the exposure time to obtain the best possible S/N. There is another way of improving the S/N based on the knowledge that the local noise decreases as the

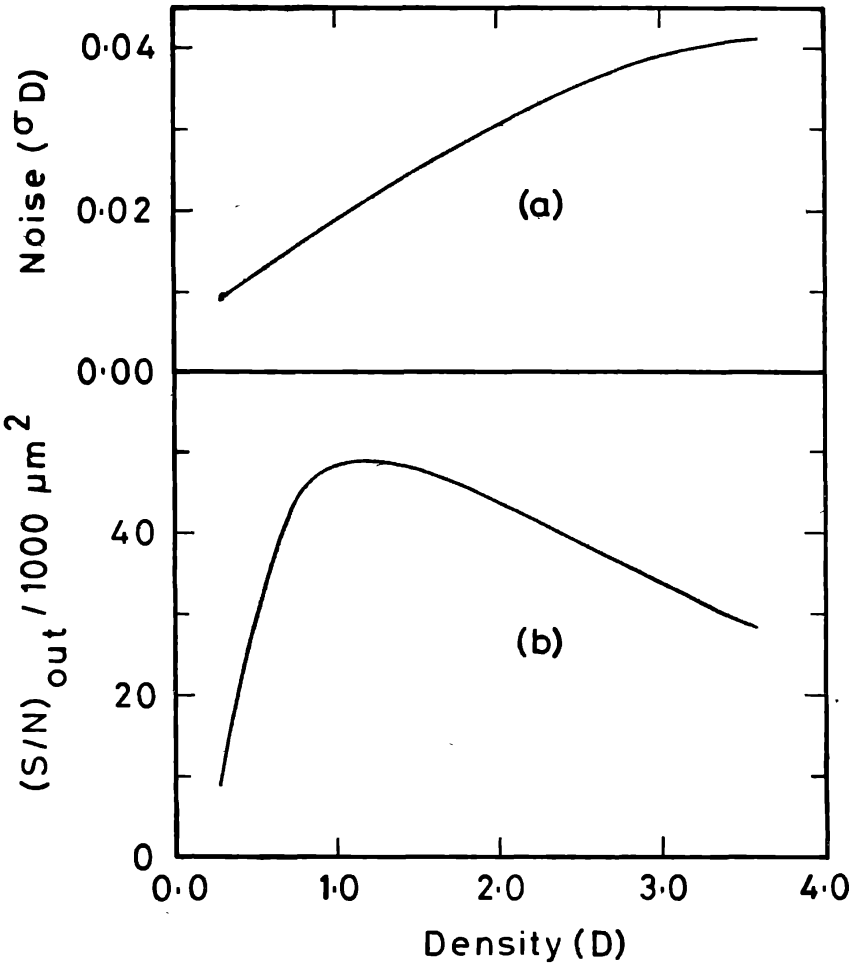

Figure 1. Typical variation of (a) the density noise and (b) the output signal-to-noise ratio with diffuse density for hypersensitized IIIa-J emulsion.

square-root of the area of the image sampled. That is, as we widen the microdensitometer slit, the number of detector elements sampled is increased, and consequently the noise reduced. Thus in order to improve the S/N, one may increase the image scale, so that an image element of interest falls over a large area of the detector. The microdensitometer slit is also enlarged correspondingly. This principle has long been employed in photographic spectrophotometry and is known as widening the spectrogram. The star image is trailed along the slit of the spectrograph so that the spectrum recorded on the photographic plate is widened perpendicular to the dispersion. The height of the microphotometer slit is increased to let in the entire width of the spectrum while scanning the plate. A 1-mm wide spectrum yields a very good S/N. More widening may deteriorate S/N because of inhomogeneities of the emulsion (increasing noise at larger spacings).

The grain noise of the emulsion also increases when hypersensitizing techniques are employed. Thus, even though the speed of an emulsion increases when hypersensitized, the output S/N decreases for a given density level. Hence one needs to balance the gain factor against the tolerable decrease in S/N. For example, when hydrogen hepersensitization is used, the speed increases until certain duration of hydrogen soaking with only a slight decrease in S/N. Once the duration is increased beyond this limit S/N deteriorates rapidly without much of a gain. Thus it is important to study the output S/N in addition to speed before making a choice of optimum conditions of hypersensitization.

3. RS CVn binaries

M. V. Mekkaden, A. V. Reveendran and S. Mohin of Indian Institute of Astrophysics Bangalore, write :

An eighth magnitude star in the constellation Canes Venatici has evoked a lot of interest in recent times. This star, RS CVn, is the prototype of a group of binaries termed RS CVn systems. Their peculiar behaviour, like the presence of strong Ca II H and K emission and photometric variation, make them interesting objects for thorough observation and analysis. These systems have the hotter component of spectral type F or G, luminosity IV or V and cooler component of late G or early K and luminosity IV. Most of them have mass ratios around unity, photometric periods between 2d and 14d and the rotational and orbital periods nearly the same.

Apart from showing photometric light variation, many of these objects have radio emission and most of them have been detected at soft x-ray wavelengths. Flare activity, both optical and radio, has been detected in a few of the RS CVn binaries, and RS CVn, UX Ari and HR 1099 have H_α in emission. The broad-band *UBV* observations by several groups show that the amplitudes and the phases of the photometric wave minima of these binaries change from time to time. Observations with the international ultraviolet explorer showed the presence of strong emission lines of O I, C I-IV, He II, N V and Lyman alpha. These lines originate from a very active chromosphere. The radial velocities derived from the Ca II H and K emission lines agree well with the velocities derived from the absorption lines of the cooler component. Hence it is beyond doubt that the activity is associated with the cooler component of the binary.

Several investigators have tried to explain the peculiar behaviour of these systems and the most suitable explanation seems to be that proposed by Douglas Hall. His model is mainly based on the assumption that the activity that is found in the cooler component can be treated as an enhanced solar-activity-like phenomenon. Dark active areas, spots, cover about 20 to 30 per cent of the stellar surface and these spots are associated with strong magnetic fields. The rotational modulation of the spots produce the wavelike distortion in the photometric behaviour of these binaries. Owing to differential rotation, the spots tend to migrate, and this migration could be identifield with the retrograde motion of the photometric wave. Because of the highly active spots we could expect strong chromospheric activity that in turn produces Ca II H and K, and H_α emissions. Spectroscopic observations prove that the dark spots on the cooler components are the cause for the peculiar behaviour of these binaries.

Continuous monitoring is essential to have a clear understanding of the level of activity of RS CVn binaries. Table 1 gives a few bright members of the RS CVn group.

Table 1. Bright RS CVn binaries

Star	Coordinates (1900)		Magnitude (Visual)	Period	Spectral type hot + cool
	α	δ		d	
	h m	° ′			
UX Ari	03 20.5	+28 21	6.40	6.438	G5V + K0IV
HR 1099	03 31.6	+00 16	5.88	2.83782	G5V + K0IV
RS CVn	13 06.0	+38 28	7.9 to 9.0	4.7978	FIV + K0IV
σ^2 CrB	16 10.9	+34 07	5.76	1.1398	F6 + G1
AR Lac	22 04.6	+45 15	6.11	1.983	G2IV + K0IV
SZ Psc	23 08.3	+02 08	7.22	3 966	F8V + K1V
HD 224085	23 49.9	+28 06	7.49	6.7242	K0IV

4. Chemical abundances in stellar atmospheres

S. Giridhar of Indian Institute of Astrophysics, Bangalore, writes :

At the beginning of the nineteenth century, Joseph von Fraunhofer compared for the first time the spectra of the sun, the planets and a few bright stars. Kirchhoff, in 1867, derived his famous laws of spectroscopy from a study of a number of laboratory sources and pointed out that the sun and the stars were extremely hot bodies of gas surrounded by cooler reversing layers. Kirchhoff's laws of spectrum analysis provide us the means of determining the chemical composition of the outer layers of stars. Later, William Huggins examined the spectra of a large number of stars. Comparing the positions of dark lines with those of bright lines emitted by laboratory sources, he identified lines of a number of terrestrial elements in the solar spectrum and concluded that matter was everywhere alike.

A new epoch in the history of spectrum analysis was inaugurated by H. A. Rowland in 1882. The flat and concave gratings designed by him provided an enormous increase in dispersion, definition and resolving power. Luckily for Rowland, the modern photographic dry plates of higher sensitivity were discovered at about the same time. The two important pieces of work by Rowland are (i) his great map of the solar spectrum and (ii) his measurements of the wavelengths of lines

in the solar spectrum and the eye estimates of their intensities. Russell, Adams and Moore pointed out in 1928 that Rowland's eye estimates of intensities of Fraunhofer lines could lead to a measurement of the chemical composition of the solar atmosphere if these estimates were calibrated for the number of absorbers. They demonstrated the large difference in the relative number of atoms effective in producing lines of different intensities in Rowland's scale. The calibration was done with the help of the multiplets in the atomic spectra, the relative strengths of whose lines could be theoretically predicted. The important outcome of this work was the establishment of the overwhelming dominance of hydrogen in the stellar atmospheres.

The eye estimate of the strength of lines was later replaced by a quantity which could be measured accurately and hence is more objective. This quantity is known as the *equivalent width* of a line. It is expressed in terms of the total amount of energy subtracted from the adjacent continuum by the absorption line. Thus the equivalent width of an absorption line is mesured by the area of the line below the continuum. The advantage of equivalent widths is that they are independent of the instrumental dispersion and resolving power.

The curve of growth

The intensity of the spectral line does depend upon the number of atoms of the element considered, but there are also other factors which effect the strength of the line. A reliable estimate of the number density of absorbers can be made only with a clear understanding of the line-forming process. Voigt, Minnaert and Slob studied the equivalent widths of lines by means of a relationship now known as the *curve of growth.* The curve of growth is a relationship between the equivalent width of a line and the number of atoms acting to produce it, or more precisely, the quantity Nf where N is the number of absorbers and f is the oscillator strength. Early calculations of curves of growth by Minnaert and Mulders (1931) and Menzel (1936) were based on Schuster-Schwarzschild (S—S) model. According to this model the stars have a photosphere which emits the continuous spectrum. Above this photosphere lies a cooler layer of gas known as the reversing layer where the entire absorption spectrum is formed. As the light of the photosphere passes through it, the dark Fraunhofer lines are formed and are superimposed on the continuous spectrum. The photosphere is assumed to absorb and emit at all frequencies like a blackbody at a given temperature. On the other hand, the reversing layer can absorb light of certain selected frequencies depending upon the composition and state of ionization and excitation of the atoms present in the reversing layer.

Later, it became apparent that this model presented an oversimplified picture. Milne and Eddington suggested a model in which all layers of stellar atmosphere contributed to the continuous as well as line absorption. For each layer, the ratio of the line to continuous absorption coefficients was considered constant. Curves of growth using Milne-Eddington (M—E) models have been constructed by Goldberg and Pierce (1948) and by Wrubel (1949) among others. Wrubel computed the curve of growth based on Chandrasekhar's exact solution of the transfer equation for the lines formed according to the M—E model. These curves of growth have been used in many abundance determinations.

The differential curve-of-growth method

Absolute curve-of-growth calculations are extremely tedious since the calculations of parameters like absorptions coefficients and broadening parameters need to be carried out for each and every line. The most serious difficulty is the requirement of precise gf values for all the lines. To circumvent these difficulties, a method is devised in which one compares the spectrum of the program star with a star for which the atmospheric parameters are precisely determined. This comparison star must be similar to the program star in its effective temperature (T_e) and surface gravity (log g). One can then assume the curves of growth for both the stars to be the same. The differences in the strengths of the lines can hence be attributed solely to the differences in the chemical compositions of the elements responsible, and thus the abundances can be determined relative to the abundances in the comparison star.

In the single-layer curve-of-growth procedure, it is supposed that all the essential properties of the spectrum can be represented by a single value of temperature and pressure. However, in reality, the lines of different excitation potentials are formed in different layers of the stellar atmosphere. Hence the variation of the physical parameters like the temperature and pressure with depth must also be taken into consideration. The methods of abundance determination which incorporate the atmospheric structure are termed collectively as the *fine analysis*. We shall discuss these methods in a forthcoming issue.

5. Lunar occultations

Lunar occultations of bright stars and Jupiter predicted for Kavalur and New Delhi have been given in tables 2 and 3 respectively. The predictions for New Delhi have been supplied by J. E. S. Singh of Nehru Planetarium, New Delhi. It may be noted that the occultations of BD + 1°212 on March 16, of HR 1954 on March 21, of γ Cancri on March 24 and of ν Virginis on March 27 and June 17 are visible from both Kavalur and New Delhi, and hence from all intermediate latitudes in India. Several stars in tables 2 and 3 have physical or optical companions. The star 11 Sagittarii has a 11.5 mag companion 42 arcsec away, γ Cancri has a nineth magnitude one 106 arcsec away, ν^2 Scorpii has a 6.5 mag one 41 arcsec away, HR 1110 has a 11.8 mag one 36 arcsec away, ϵ Capricorni has a 9 mag companion 68 arcsec away, and τ^2 Aquarii a 9 mag one 132 arcsec away. Several stars have been discovered by occultation techniques to be close pairs : 82 Geminorum (difference in magnitudes = 0.1, separation = 0.3 arcsec), η Leonis (0.5 mag, 0.097 arcsec), ν^2 Scorpii (2.0 mag, 0.0003 arcsec; 2.9 mag, 1 arcsec) HR 1110 (0.0 mag, 0.3 arcsec) and ϵ Capricorni (1.3 mag, 0.047 arcsec). HU Tauri is an eclipsing variable (5.9–6.7 mag) with a period of 2.056 d; the separation is detectable by occultation observations with the highest time-resolution. The diameter of ν Virginis has been determined by such techniques to be 0.00565 arcsec. This star also shows variability with an amplitude of 0.08 mag. The barium star ω Geminorum varies by 0.09 mag with a period of 0.728 d, because of pulsations. Another variable in the list is 38 Arietis, which is a δ Scuti variable (5.18–5.22) with two periods (0.046 and 0.061 d). ϵ Capricorni is a shell star.

The lists in tables 2 and 3 do not include reappearances unless they are preceded by an observable disappearance. Two of the important reappearances are those of

Table 2. Lunar occultation predictions for Kavalur

Date 1983		Time (UT) h	m	s	Phenomena	Star or Planet	Mag.	Sp. T.	α 1983 h	m	s	δ °	′	″	Altitude deg.	Percentage illumination
March	7	21	15	31	D	11 Sagittarii	5.0	K0 III	18	10	40.1	−23	42	21	13	37−
		22	19	39	R										26	
	10	23	57	31	D	−21° 5844	7.1	F5	20	49	53.7	−21	22	40	17	12−
	16	13	57	59	D	+ 1° 212	6.7	G5	1	7	5.4	1	54	06	21	3+
	18	13	47	44	D	38 Arietis	5.2	A7III-IV	2	44	00.5	12	22	23	45	15+
		14	44	18	R										18	
	20	16	27	08	D	HU Tauri	5.9	B1V	4	37	14.6	20	39	04	19	34+
		17	19	13	R										7	
	21	18	52	37	D	HR 1954	6.4	K2	5	41	1.7	22	39	11	0	46+
	22	19	27	14	D	+23° 1486	7.4	K2	6	44	21.1	23	39	54	6	58+
	23	19	45	44	D	82 Geminorum	6.2	G2III + A4V	7	47	32.9	23	11	03	15	69+
	24	15	35	00	D	γ Cancri	4.7	A1V	8	42	18.7	21	31	49	80	78+
		17	02	31	R										64	
	26	18	18	11	D	+13° 2302	6.8	A2	10	45	26.3	12	50	12	25	94+
	27	15	42	01	D	ω Virginis	5.4	M3III	11	37	36.0	8	13	37	55	98+
		21	13	36	D	ν Virginis	4.0	M1III	11	45	00.1	6	37	23	45	99+
		22	20	33	R										28	
April	6	21	07	29	D	HR 7825	6.2	M1III	20	28	30.8	−22	26	58	7	35−
		22	09	32	R										21	
	22	14	33	54	D	42 Leonis	6.1	A1V	10	20	56.1	15	03	41	82	75+
		14	17	24	D	+16° 2116	7.4	G5	10	21	49.8	15	25	50	78	75+
		18	38	41	D	+15° 2206	7.1	K0	10	27	54.7	14	25	50	40	76+
	23	17	53	25	D	+09° 2482	6.7	A2	11	20	58.2	9	15	39	62	85+
		20	30	42	D	+ 9° 2494	6.8	K0	11	25	26.0	8	45	08	25	86+
	24	15	35	36	D	+ 4° 2583	6.8	A0	12	10	49.0	4	08	56	17	92+
	25	23	09	35	D	− 2° 3651	7.5	K2	13	12	29.7	−3	24	23	8	98+
	26	20	02	38	D	− 7° 3748	6.7	K0	13	59	11.9	−8	04	53	59	100+
May	7	23	56	13	D	HR8921	6.2	K0	23	28	07.1	−9	21	39	37	24−
	16	12	58	38	D	ω Geminorum	5.2	G6I-II	7	01	21.8	24	14	28	49	17+
		13	51	28	R										37	
		15	06	06	D	+24° 1531	6.9	M0	7	06	13.9	24	11	47	21	18+
		16	03	27	R											
	19	13	38	28	D	η^1 Leonis	3.5	A0I	10	06	24.6	16	50	47	81	50+
		14	15	21	R										72	
	23	22	13	30	D	−5° 3762	6.9	A3	13	46	33.1	−6	37	21	2	91+
	24	22	44	00	D	HR 5455	6.2	F5V	14	36	06.7	−12	14	08	4	96+
	25	22	35	41	D	ζ^1 Librae	5.6	K5III	15	27	19.2	−16	39	35	16	99+
		23	44	50	D	ζ^3 Librae	5.9	K0	15	29	44.2	−16	33	13	1	99+

May	26	16	04	49	D	ν^2 Scorpii	4.0	B3V	16	11	0.19	−19	25	07	40	100+
		17	24	16	R										53	
		22	12	30	D	Jupiter	−2.1		16	17	54.7	−20	26	53	30	100−
		22	34	22	R										25	
June	1	23	08	49	D	ϵ Capricorni	4.7	B3V	21	36	08.5	−19	32	29	57	68−
	17	17	04	02	D	ν Virginis	4.0	M1III	11	44	59.5	6	37	28	27	48+
		17	47	42	R										16	
	19	15	24	32	D	−3° 3462	7.1	K0	13	23	34.2	−4	13	15	67	70+
	20	20	32	24	D	−9° 3915	7.4	A2	14	20	39.4	−10	17	44	7	80+
	24	22	12	39	D	−24° 13521	7.1	K0	17	47	57.0	−24	12	10	23	100+
	29	23	53	05	G	−17° 6451	7.4	G5	22	07	32.1	−16	37	28	53	82−
	30	17	50	28	D	τ^2 Aquarii	4.0	M0III	22	48	42.7	−13	40	49	9	
		19	00	45	R										25	

Table 3. Lunar occultation predictions for New Delhi

Date 1983		Time (TU)			Pheno-mena	Star or Planet	Mag.	Sp. T.	α 1983			δ 1983			Alti-tude deg.	Percentage illumina-tion
		h	m	s					h	m	s	°	′	″		
March	16	13	45	11	D	+1° 212	6.7	G5	1	07	05.4	1	54	06	10	3+
	19	14	24	00	D	HR 1110	6.2	K0III	3	38	26.8	16	28	52	37	24+
	20	15	06	13	D	+90° 740	7.3	F8	4	34	39.2	19	56	03	42	34+
	21	18	22	19	D	HR 1954	6.4	K2	5	41	01.7	22	39	11	14	46+
	22	19	38	11	D	+23° 1491	6 5	G5	6	45	08.3	23	23	24	11	58+
	24	15	38	56	D	γ Caneri	4.7	A1V	8	42	18.7	21	31	49	82	78+
	27	20	58	31	D	ν Virginis	4.0	M1III	11	45	00.1	6	37	23	46	99+
April	17	14	56	09	D	109 Tauri	4.1	G8III	5	18	14.1	22	04	42	30	20+
	29	17	10	33	D	Jupiter	−2.0		16	31	09.0	−20	55	49	17	93+
		18	20	17	R										28	
May	16	15	00	58	D	+24° 1531	6.9	M0	7	06	13.9	24	14	47	28	18+
	26	21	24	17	D	Jupiter	−2.1		16	17	55.8	−20	26	56	29	100−
		22	42	22	R		−2.1		16	17	54.1	−20	26	52	16	100−
June	13	14	25	07	D	82 Geminorum	6.2	G2III + A4V	7	47	31.9	23	11	05	21	8+
	15	17	00	29	D	+17° 2156	7.4	K0	9	56	37.8	16	32	28	11	26+
	17	16	27	49	D	ν Virginis	4.0	M1III	11	44	59.5	6	37	28	35	48+

M 8 and M 28 occuring in May. The globular cluster M 28 (1983 position : $18^h\ 23^m\ 32^s.6$; $-24°\ 52'\ 55''$) will reappear from the dark edge of moon at $21^h\ 36^m\ 20^s$ UT of May 1 as seen from Kavalur. The occultation will last for about 24 minutes. M 28 has a visual magnitude of 7.3. The Lagoon nebula M8, (1983 position : $18^h\ 03^m\ 39^s.0$; $-24°\ 19'\ 53''$) will reappear from the dark edge of nearly full moon on May 28 at $21^h\ 32^m\ 06^s$ UT as seen from Kavalur. The partial stage of this seventh magnitude nebula lasts 339 minutes. The predicted times of occultation for M8 as well as for M 28 refer to the coordinate centre. The member stars of the rich open cluster embedded in M 8 will reappear one after another during the partial stage of the occultation. The brightest stars 7 and 9 Sagittarii will reappear at $20^h\ 04^m\ 27^s$ and $21^h\ 03^m\ 48^s$ respectively.

Jupiter is undergoing a series of occultations in which the ones on April 29 and May 26 will take place at night and would both be visible from New Delhi. One can observe only the latter one from Kavalur. The larger satellites of Jupiter present a disk of a few seconds of arc in diameter and hence it would be a good experience to measure their sizes by timing the duration of occultation.

The grazing occultation of BD $-17°$ 6451 on June 29 is visible only from a thin belt with the northern boundary passing through Mercara and Bangalore, and ending a little north of Madras.